Journal of Building Engineering 68 (2023) 106111

Contents lists available at ScienceDirect

Journal of Building Engineering

journal homepage: www.elsevier.com/locate/jobe

Performance of prototype tandem UV filter and organic transparent photovoltaic windows

Joaquim Romaní [a,*], Alejandro Pérez-Rodríguez [a,b], Jaume Salom [a]

[a] Catalonia Institute for Energy Research (IREC), Jardins de les Dones de Negre, 1, 08930, Sant Adrià De Besòs, Barcelona, Spain
[b] Departament d'Enginyeria Electrònica i Biomèdica, IN2UB, Universitat de Barcelona, Barcelona, Spain

ARTICLE INFO

Keywords:
Solar energy
Transparent BIPV
Building simulation
Renewable energy
Photovoltaic
PV glazing

ABSTRACT

Building integrated photovoltaics (PV) are promising technologies to integrate renewable energy production and achieve positive energy buildings. Transparent photovoltaics increase the integration options, especially in windows and skylights. In this context, the Tech4win project has developed a prototype tandem UV filter and organic transparent photovoltaic. The current paper presents a techno-economic analysis of the performance of this prototype. The laboratory data is introduced in a TRNSYS18 simulation for evaluating the impact in the heating, cooling, lighting, and the PV electrical production. The simulation scenarios include office and residential buildings in five different climates. Moreover, the economic analysis consists of a sensitivity study on the PV window investment cost, the electricity price, and the feed-in tariff. The results show that the PV windows increase the heating and lighting demand in all cases, but may decrease the cooling demand compared to non-solar control windows. Consequently, in the heating dominated scenarios the PV windows increase the energy demand but, in cooling dominated cases, the demand only decreases if the PV window's solar heat gain coefficient (SHGC) improves that of conventional window. Nevertheless, in all studied scenarios the PV window improved the building energy balance. Finally, the electricity pricing schedules and the feed-in tariff are key into the economic feasibility.

Nomenclature

Abbreviations

AVT	Average visible transmittance
BIPV	Building integrated photovoltaics
BSDF	Bidirectional scattering distribution function
CAPEX	Capital expenditures
CF	Cash flow
CFS	Complex fenestration system
CRI	Colour rendering index
DPP	Discounted Payback Period
IR	Infrared

* Corresponding author.
E-mail address: jromani@irec.cat (J. Romaní).

https://doi.org/10.1016/j.jobe.2023.106111
Received 8 November 2022; Received in revised form 8 February 2023; Accepted 12 February 2023
Available online 17 February 2023

Table 1
Summary of BIPV simulation studies windows properties.

Ref.	Climates	BIPV window	Reference window
[10]	Los Angeles (as reference for southern Italy)	a-Si:H and perovskite cells double pane window a-Si:H U = 2.725 SHGC = 0.398 T_{vis} = 0.274 Perovskite U = 2.725 SHGC = 0.491 T_{vis} = 0.388	Double pane clear glass window (air gap) U = 2.725 SHGC = 0.804 T_{vis} = 0.828
[19]	Harbin Beijing Shanghai Guanzhou Kunming	Thin film CdTe on double glazed unit U = 2.54 SHGC=NA T_{vis} = 10%	Clear double-glazing pane U=NA SHGC=NA T_{vis} = NA
[20]	Harbin Beijing Shanghai Guanzhou Kunming	Thin film 10% transparency CdTe on double glazed unit U = NA SHGC = NA T_{vis} = 10%	Clear double-glazing pane U=NA SHGC=NA T_{vis} = NA
[15]	New Damietta	Single pane a-Si U = 2.783 W/m2K SHGC = 0.367 T_{vis} = 40%	Single clear glass U = 6.121 SHGC = 0.81 T_{vis} = 88%
[17]	Taiyuan	a-Si Single-layer glass Double-layer glass U=NA SHGC=NA T_{vis} = NA	Single-layer clear glass double-layer clear glass U=NA SHGC=NA T_{vis} = NA
[16]	Harbin Beijing Shanghai Hong Kong Kunming	a-Si double pane insulated glazing With clear glass: U = 2.635 SHGC = 0.220–0.329 T_{vis} = 0.100–0.260 With low-e glass: U = 1.621 SHGC = 0.220–0.329 T_{vis} = 0.138–0.212	Double layer with tined and clear glass U = 2.699 SHGC = 0.501 T_{vis} = 0.473
[21]	Harbin Shanghai Guangzhou	Double glazing 10% CdTe 50% CdTe Flat silicon U=NA SHGC=NA T_{vis} = NA	Double glazing with float glass U=NA SHGC=NA T_{vis} = NA
[25]	Detroit Los Angeles Phoenix Honolulu	Double glazing Organic cell U=NA SHGC=NA T_{vis} = NA	Double clear glazing U=NA SHGC=NA T_{vis} = NA
[26]	Oslo Chicago Dhaka Abu Dhabi	Non-wave-length silicon. Single STPV glazing and double-glazing with low-e glass. U = 1.0–5.6 SHGC = 65% T_{vis} = 50%	NA.
[24]	Chengdu Chongqing Guiyang Lhasa Kunming	c-Si cell cladding on double-glazing.	NA.
[22]	Hyderabab	CdTe Single glazing. U = 5.678 SHGC = 0.210–0.275 T_{vis} = 0.252–0.327 Double glazing:	Same optic-thermal properties as BIPV windows but without PV output.

(continued on next page)

Table 1 (*continued*)

Ref.	Climates	BIPV window	Reference window
		$U = 1.812$ $SHGC = 0.228–0.271$ $T_{vis} = 0.229–0.297$	
[27]	Oslo Dhaka Abu Dhabi	Perovskite ($CH_3NH_3PbI_3$) Single and double-glazing with low-e coating. $U = 2.9$ $SHGC = 43.2\%$ $T_{vis} = 40\%$	Clear single glass and insulated glass. SHGC and Tvis equal to PV window. $U = 1.0–5.9$ $SHGC = 43.2\%$ $T_{vis} = 40\%$
[23]	Hothot Tianjin Hefei Kunming Xiamen	CdTe cell. Double-glazing in insulated and vacuum glass structures. $U = 1.145–2.667$ $SHGC = 0.152–0.261$ $T_{vis} = 0.142–0.159$	Single and double clear glass. $U = 2.696–5.753$ $SHGC = 0.787–0.877$ $T_{vis} = 0.818–0.901$
[18]	Sheffield	Different models of a-Si, c-Si and CdTe. Double glazing units. a-Si $U = 2.783$ $SHGC = 0.145–0.367$ $T_{vis} = 0.01–0.26$ c-Si $U = 3.5$ $SHGC = 0.25$ $T_{vis} = 0.42$ CdTe $U = 1.182$ $SHGC = 0.129–0.271$ $T_{vis} = 0.06–0.275$	Double clear glass. $U = 2.761$ $SHGC = 0.761$ $T_{vis} = 0.812$

NPV	Net present value
OPEX	Operational expenditures
OPV	Organic PV
PV	Photovoltaics
SHGC	Solar heat gain coefficient
TPV	Transparent BIPV
T_{vis}	Visible transmittance
U/U-value	Thermal transmittance
UV	Ultraviolet
β_T	PV efficiency thermal coefficient
η_{ref}	PV nominal efficiency

1. Introduction

Improving the energy performance of buildings is one of the biggest challenges that society faces in order to steady the increasing global average temperature to just 1.5 °C above pre-industrial levels [1]. IEA estimations show that buildings represent 36% of final energy consumption and 39% of energy and process related CO_2 emissions [2]. Moreover, the energy consumption is expected to keep rising mainly due to the growth of the built environment (2.5% per year), but also due to increase in air-conditioner ownership and extreme weather events [3]. Consequently, policymakers are issuing regulations to improve the building's energy efficiency and make them net zero or positive energy buildings. For example, the European Commission issued the EU Energy Performance of Buildings Regulation [4] and the Energy Efficiency Directive [5]. According to the regulations, in order to achieve these goals, improvements in the building envelope and the integration of renewable energy technologies is essential. Depending on the climate and design, among the other elements of the building, inefficient windows can contribute to between 20 and 40% of a house total energy use [6] as they usually represent a significant share of a building envelope (especially for office buildings). Due to this, the development of transparent and semi-transparent photovoltaics has risen the interest in building integrated photovoltaic (BIPV) windows, as discussed in the most recent reviews [7–11].

BIPV are PV modules integrated in the building envelope by replacing conventional building materials [12]. Therefore, BIPV allow for on-site renewable energy generation while they are aesthetically integrated and they affect the building energy behaviour. The most common BIPV solutions use silicon cells, which are integrated in the opaque part of the envelope (walls and roof) as tiles, foils, or modules. A usual challenge of BIPV on the opaque sections is dealing with the high temperatures of the cells, which often lead to photovoltaic thermal (PVT) solutions to harvest the heat of the BIPV system for heating and ventilation. Nevertheless, BIPV can also be implemented into the transparent parts of the envelope (windows and skylights). Opaque cells, usually silicon based, are integrated in the window as cell cladding, which form a pattern of opaque and transparent sections. However, the development of amorphous stabilized silicon (a-Si), cadmium telluride (CdTe), copper indium gallium selenide (CIGS), dye-sensitized, perovskites, and organic transparent or semi-transparent technologies [13] has risen the interest because it capabilities for integration in BIPV windows.

Windows have a significant impact on the building energy behaviour. The thermal transmittance (U-value) of windows is usually lower than that of the opaque sections of the envelope. Moreover, windows allow solar radiation to enter the building. On one side, the visible transmittance (T_{vis}) influences the optical comfort (illuminance level and glare) and daylighting, hence the artificial lighting energy use. On the other side, solar heat gain coefficient (SHGC) determines the solar heat gains of the buildings, which are key to the heating and cooling demand. As a result, the design of a building envelope requires balancing the window properties (U-value, T_{vis}, and SHGC) as well as their size and orientation in order to minimize the heating, cooling, and lighting demand, while maintaining good thermal and optical comfort. BIPV windows add the electrical output into the optimization problem, which requires a multifactorial analysis. This complexity has led to the development of different simulation models for BIPV windows [11].

Recent simulation studies on the impact of BIPV windows into the building energy performance studied mainly the behaviour in different climates, impact of the window-to-wall ratio (WWR), and daylighting. with some research introducing model validation and life cycle analysis (LCA). The technologies researched include prototypes and commercial products, with the focus being on a-Si [14–18] and CdTe [18–23] while c-Si [18,21,24], perovskites [14,19], and organic [25] PV cells are also introduced. Overall, the research highlights the solar and daylighting control properties of BIPV windows [14,15], with a high potential for energy savings in all the climatic regions investigated. These include cities as close to the equator as Hyderabad (India) (17° N) [22] and as far as Oslo (Norway) (59°N) [23,26]. Several studies emphasized the relevance of the window-to-wall ratio (WWR), highlighting that the BIPV windows increase the energy savings advantages over conventional windows the higher the WWR [18–20,22,23,26,27]. The good energy results were complemented by good LCA results [24,25] and the evaluation of nearby shadows and clouding highlighted the increasing relevance of these parameters at higher latitudes [26]. Noticeably, the reviewed literature did not consistently report the windows thermal and optical properties, as summarized in Table 1. Moreover, the reference conventional windows consisted mostly of clear or low-e glass in single or double glazing configurations. Solar control windows, adequate for warm climates and highly glazed buildings, or triple glazing windows for cold climates would be interesting reference windows in most scenarios. Furthermore, the local building regulations may impose minimum specifications on the windows characteristics, which will affect the implementation of BIPV windows.

The present article analyses the impact of a prototype transparent PV glass into the building energy performance. The PV glass prototype is developed within the Tech4win project [28] and it consist of a tandem structure of organic photovoltaic (OPV) cell [29] and PV active UV filter [30]. The main research question is to evaluate whether the PV glass prototype has a positive impact in the building energy balance and in which conditions it will be economically feasible. The research gap motivating this question is the need to evaluate the performance of this new prototype PV window. Additionally, the current article also covers two research gaps in the topic of transparent PV windows modelling and evaluation: 1) Economic evaluation methodology, identifying the parameters that most influence the performance; 2) Comparison of the PV window to adequate conventional windows. As observed in the literature review, very few have included an economic evaluation. Moreover, the conventional reference windows selection is debatable in some cases. For example, there is total absence of solar control windows. The novelty of the research is: i) A prototype PV glass, with data obtained from laboratory level assuming best and lower efficiency scenarios; ii) Economic evaluation dependent on electricity pricing schedules and scenarios; iii) Definition of window solutions (both conventional and PV) adequate to the location, considering the local

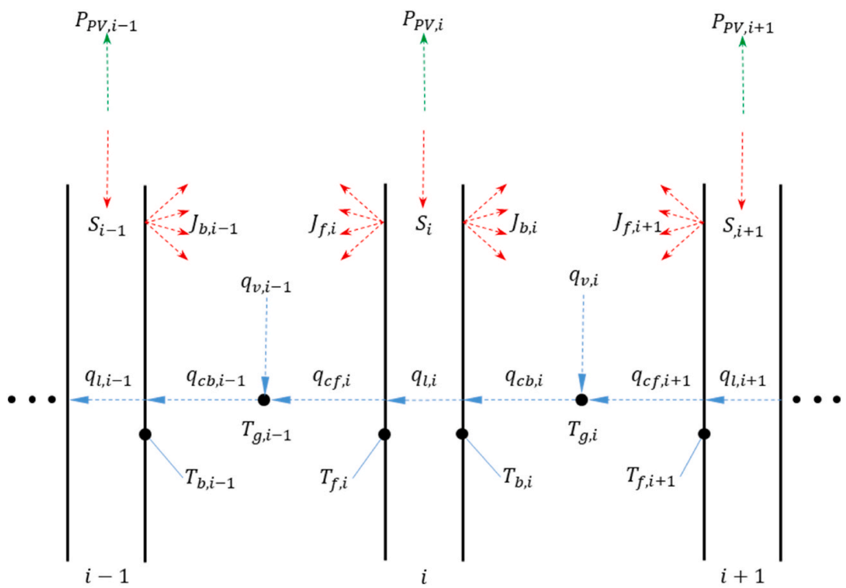

Fig. 1. Modified ISO 15099 glazing system energy balance from Romaní et al. [32].

building regulations.

Accordingly, the article is structured as follows. Section 2 presents the methodology, including a summary of the modelling with TRNSYS18 and the evaluation framework. Section 3 presents the case of studies, describing the two buildings modelled (residential and office cases) and the locations. The latter determine the climatic conditions and the building regulations, which are used to define the building envelope characteristics and the windows configuration. Section 4 presents the summary of the results, which are further discussed in Section 5 and closed with the conclusions in Section 6.

2. Methodology

2.1. Modelling

The simulations are carried out with TRNSYS18 [31], a graphical based software environment used to simulate the behaviour of transient systems. The methodology follows the modelling approach presented in Romaní et al. [32], which is based on Type 56 detailed multi-zone building and it simulates the transparent photovoltaic (TPV) window using a modified version of the complex fenestration system (CFS). The combination of the Type 56 and the modified CFS add-on allow to make an integrated simulation of the heating, cooling, and lighting demand. The modified CFS model uses the bidirectional scattering distribution function (BSDF) for optical calculations and the ISO 15099 (2003) [33] for energy balance calculation. The BSDF is used to calculate the available radiation at the PV cell position. Then the PV output is calculated with equation (1) and introduced in the modified energy balance of the window, as presented in Fig. 1. The details on the model verification and parameters selection is presented in Romaní et al. [32].

$$\dot{P}_{PV.i} = \eta_{ref}\left[1 + \beta_T\left(T_i - T_{ref}\right)\right] G_{\tau\alpha} \quad \text{(eq. 1)}$$

Where: $\dot{P}_{PV.i}$: PV output at "i" window pane [W·m^{-2}]; η_{ref}: PV cell nominal efficiency [−]; β_T: Temperature coefficient [%·K^{-1}]; T_i: temperature of the window pane [°C]; T_{ref}: reference temperature of PV cell nominal efficiency calculation (25 °C); $G_{\tau\alpha}$: transmitted and absorbed solar radiation at the window pane "i" [W·m^{-2}].

Finally, the daylight conditions of the zones are calculated with the DaySIM approach inbuilt to TRNSYS Type 56 [34]. This requires defining sensors points inside the zones, for which the illuminance conditions are evaluated according to the incident solar radiation, geometry of the room, reflectivity of the walls, and windows properties.

The modelling approach was used before on a preliminary evaluation of the impact of TPV into office buildings in Spain [35].

2.2. Evaluation indicators

2.2.1. Energy

The BIPV windows have an impact in the heating, cooling, and lighting energy use buildings. Moreover, the BIPV generate electricity that further impact the building energy balance. Hence, the energy performance of the buildings is evaluated in terms of total final energy demand and final energy demand balance. On one side, the total energy demand accounts the sum of heating, cooling, lighting, ventilation, and equipment loads. On the other, the energy balance subtract the PV output from the total energy demand. Note that the energy balance does not consider whether the PV output is self-consumed by the building or exported to the grid.

$$E_{\{demand\}} = E_{\{heating\}} + E_{\{cooling\}} + E_{\{lighting\}} + E_{\{ventilation\}} + E_{\{equipment\}} \quad \text{(eq. 2)}$$

$$E_{\{balance\}} = E_{\{heating\}} + E_{\{cooling\}} + E_{\{lighting\}} + E_{\{ventilation\}} + E_{\{equipment\}} - E_{\{photovoltaics\}} \quad \text{(eq. 3)}$$

2.2.2. Daylighting

The daylighting is measured with the average illuminance of different sensor points distributed in the reference rooms of the case studies. The performance is calculated as the fraction of occupancy hours in which the room is above the minimum required illuminance (depending on the case study) and above 2000 lux, the threshold in which occupants may experience discomfort according to the upper limit set by the useful daylight illuminance (UDI) indicator [36,37].

2.2.3. Economic

The study evaluates the performance of a prototype PV glazing, hence the current technology development level makes difficult to assess the technology cost. In this context, the economic evaluation is carried out as a sensitivity analysis of the discounted payback period (DPP). It is calculated as the number of years that are required to achieve a net present value (NPV) above zero. The NPV is calculated according equation (4), in which the capital expenditure (CAPEX) of the PV window and the average electricity price are the independent variables of the sensitivity study. The business case assumes a refurbishment scenario in which the windows need to be replaced, hence comparing the investment and operation cost of the conventional versus the PV window. In this scenario, the CAPEX in equation (4) is the difference between the investment costs of the windows. The cash flow (CF), see equation 7, accounts the difference of the operation cost of the conventional window and the PV window, taking into consideration the incomes that may be generated by electricity exports.

$$NPV = \sum\nolimits_{i=0}^{N} \frac{CF_i(1+p)^i}{(1-d)^i} - CAPEX \quad \text{(eq. 4)}$$

$$CF_i = OPEX_{conv.i} - \left(OPEX_i - Incomes_i\right) \quad \text{(eq. 5)}$$

where: NPV, net present value; CF, cash flow; CAPEX, capital expenditures; OPEX, operational expenditures; 'N', number of years; 'i', year; 'd', discount rate; 'p', electricity price change rate.

The OPEX calculation accounts only for the cost of electricity, excluding the maintenance and the replacement cost. The schedule of the electricity tariff is a relevant parameter into the feasibility of PV windows. Therefore, two electricity price schedules are used. On one side, the "current" electricity hourly tariff schedule in Spain is used. It is a demand following profile that distinguishes between "peak", "flat" (intermediate), and "valley" (low) periods. On the other side, the high penetration of photovoltaics made the California Independent Operator to publish the "duck" chart in 2013 [38]. In order to encourage the use of renewables, the duck chart has a "super-valley" price at mid-day hours. The "current" and "duck" chart electricity price schedules are adapted from Syn.ikia project [39] and its profiles are shown in Fig. 2. In order to ease the comparison in the sensitivity analysis, the average electricity price is used to calculate the "current" schedule "peak", "flat", and "valley" tariffs. Then, the "duck" chart scenario uses the same range of prices with the "super valley" tariff being calculated proportionally. Consequently, the effective average electricity price of the "duck" scenario is lower.

The study does not consider any energy storage, hence the feed-in tariff are a key parameter to determine the feasibility of any PV system that may have overproduction. As compensation scenarios are very variable, depending on country regulations and specific contracting conditions, three scenarios are considered: no-compensation (feed-in tariff of 0%); compensation at 30% of the simultaneous electricity price; and net-metering, compensating at 100% of the electricity price. In any case, the monthly bill is not allowed to be negative. Finally, the discount rate and an average electricity price increase are fixed to 5% and 1.2%, respectively.

3. Cases of study

The study aims to evaluate the performance of the PV glazing in glazing systems that fulfil the requirements for different type of buildings and climates. The current section describes the selected locations, type of buildings, and the characteristics of the PV window implemented in each case.

3.1. Location

The location defines the meteorological conditions, the building requirements, and the reference electricity price for the economic study. Five different location in three different countries are selected to cover diverse climates. Denmark is a reference for a heating dominated climate; Spain represents and intermediate climate with both cooling and heating demand; and India represents a cooling dominated climate. Furthermore, the building regulation in Denmark [40] considers only a single climatic zone, but Spain [41] and India [42] divide the country in different climatic regions, each having different building energy performance requirements. Hence, for Spain and India the study considers two different climatic regions. Köppen Geiger [43] climatic classification is used to verify to ensure a diversity of climatic conditions. Finally, the climatic data used in the simulation are typical meteorological year (TMY) obtained from the Meteonorm8 database [44] for representative cities within the selected climatic regions, as summarized in Table 2.

3.2. Buildings types

The performance of the BIPV glazing is evaluated in both office and residential buildings. This section summarizes the geometric characteristics of the buildings, the envelope parameters, the occupancy profiles, the internal gains, and the operation regimes. Note that the characteristics of the windows are described in a specific section.

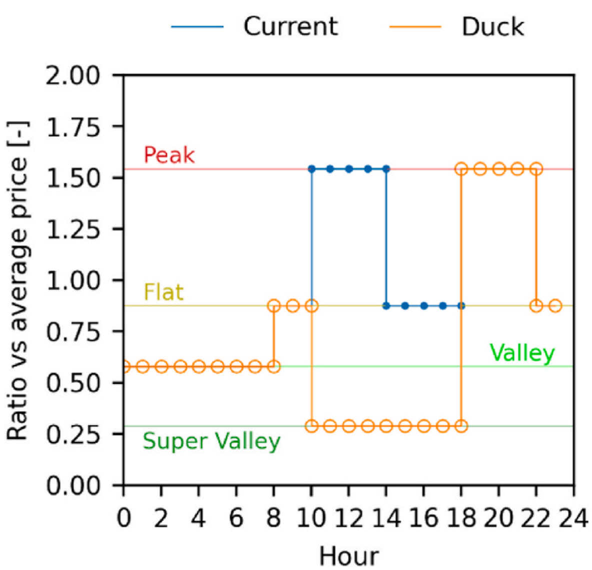

Fig. 2. Current and future electricity price schedules [39].

Table 2
Reference cities for climatic data summary.

Climate	Meteonorm reference city	Building regulation climate	Köppen Geiger classification	Lat.	Long.	Alt.	T_{avg} [°C]	I [kWh/m^2]
København	København/Taastrup	Denmark (single zone)	Cfb (oceanic climate)	55.67	12.3	12.3	9.1	979.3
León	León/Virgen del Camino	E1	Csb (Warm-summer Mediterranean climate)	42.58	−5.65	914	12.3	1610.4
Almería	Almería Airport	A4	BWh (Hot desert climate)	36.85	−2.38	21	18.4	1831.3
Bangalore	Bangalore	Moderate	Aw (Tropical savannah climate)	12.97	77.59	912	23.7	2015.4
New Dehli	New Delhi	Composite	BSh (Hot semi-arid climate)	28.58	77.21	212	24.8	1963.4

3.2.1. Office

A reference room from a real office building is used a reference for this study, as shown in Fig. 3. The building is model is taken from previous research in which validation with experimental data was carried out [45]. The geometric characteristics are summarized in Table 3 and the envelope characteristics are summarized in Table 4. The details of the surfaces characteristics are described inAppendix A. The room only has one exposed façade facing south.

The occupants and equipment internal gains, as well as set-points and ventilation regimes are driven by the occupancy schedule, which is shown in Fig. 4. The lighting gains are driven by a daylighting control in which lights are continuously dimmed between zero daylight illuminance and a set-point of 500 lux during hours with occupancy, as shown in Fig. 5.

The values for the internal gains and their associated electricity consumption are calculated according to ASHRAE fundamentals [46] and are summarized in Table 5. The equipment and people gains assume nine people working with desktop computers. Lighting gains consider LED lights with a target illuminance of 500 lux at a working plane at 0.85 m from the floor. The ventilation air changes at full occupancy are 1.2 h^{-1} while infiltration is assumed constant at 0.32 h^{-1}.

During occupancy periods, the HVAC operates under the set-points summarized in Table 6. During non-occupancy hours the heating system dials down to a set-back, while cooling and dehumidification are turn off. The HVAC consists of fan coils fed by a reversible heat pump with a heating coefficient of performance (COP) of 3.5 and a cooling energy efficiency ratio (EER) of 2.2.

3.2.2. Residential

The residential building used as case of study is taken from a representative archetype of residential buildings in Spain, specifically Type D from Joana Ortiz doctoral thesis [47]. It was developed within MARIE project [48] and it is comparable to the archetypes presented in the TABULA database [49]. It is a semi-detached house of three floors with the South and North façades exposed, as presented in Fig. 6. The geometric and envelope characteristics are summarized in Table 7 and Table 8, respectively. The details on the surface characteristics are presented in Appendix B.

The load regimes of the residential building are driven by the occupancy. A stochastic model [50] validated with use of time statistics [51] is used to describe the occupancy profile of a four people family for a home with high use of appliances. The model determines at each time step the number of people in the house, the use of appliances, and the location in the house. The use of appliances is simplified to an active/no-active equipment and it influences the equipment internal gains. The location in the house distribute the occupants between the day zone (from 7 h to 23 h) and night zones. A single occupancy profile was generated with the stochastic model and used in all the residential building simulation to guarantee consistency and comparability of the results. Fig. 7 shows the occupancy schedule of a sample day of the stochastics occupancy model.

The internal gains are calculated according ASHRAE Fundamentals [46], assuming light sedentary and sleep type of internal gains for daytime and night periods, respectively. The internal gains are distributed uniformly among all the day or night zone, depending on the occupancy schedule. During "non-active" period, the gains are distributed among the night zones, but among day zones during "active" periods. Lighting gains assume compact fluorescent light controlled under and ON/OFF strategy with a turn ON set-point of <100 lux and a turn OFF set-point of 200 lux, but only if there is occupancy in the room. The remaining appliances internal gains are considered constant if there is active occupancy. Table 9 summarizes the internal gains characteristics and the associated electricity consumption.

During occupancy periods, the HVAC operates under the set-points summarized in Table 10. During non-occupancy hours, the heating system dials down to a set-back. The HVAC consists of fan coils feed by a reversible heat pump with a heating coefficient of performance (COP) of 3.5 and a cooling energy efficiency ratio (EER) of 2.2.

3.3. Windows

The study aims to investigate the impact into the building's energy performance of a prototype of transparent photovoltaic glazing from the Tech4win project [28]. The prototype consists of a tandem structure of a photovoltaic active UV filter and IR organic

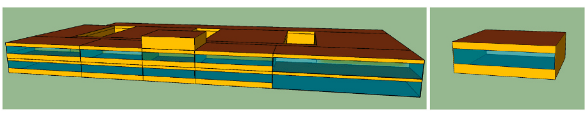

Fig. 3. Office building reference room, complete building view (left) and the room isolated (right).

Table 3
Office building reference room geometric characteristics.

Parameter	Value
Length	11.21 m
Depth	9.58 m
Height	3.47 m
Floor surface	107.39 m^2
Façade surface	33.24 m^2
Window surface	18.48 m^2
Window to Wall Ratio (WWR)	47.5%

Table 4
Office building reference room external wall characteristics.

Climate	U [W/m^2K]
København	0.180
León	0.307
Almería	0.687
Bangalore	0.436
New Delhi	0.392

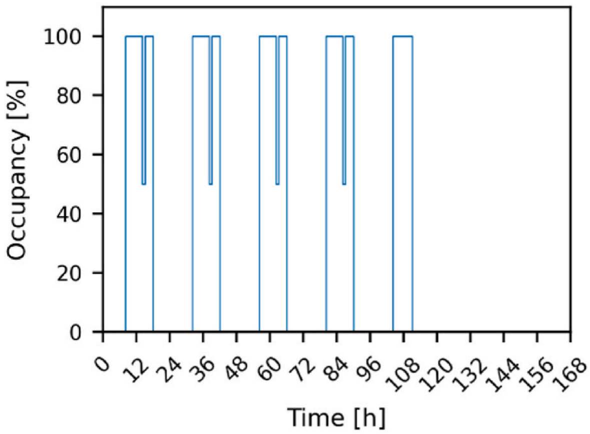

Fig. 4. Office building occupancy schedule.

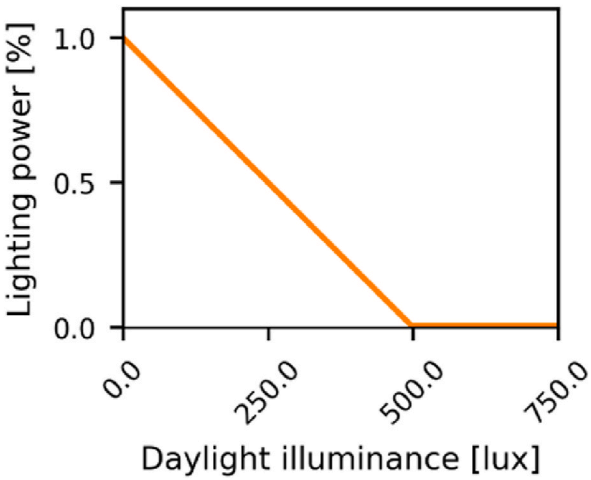

Fig. 5. Office building continuously dimming daylighting control.

Table 5
Office heat gains and associated electricity consumption.

Type	Sensible gain [W/m^2]	Radiative fraction [−]	Latent gain [kg·s^{-1}·m^{-2}]	Electricity consumption [W/m^2]
Equipment	4.5	0.2	–	5.625
People	6.0	0.5	1.799 ·10-6	–
Light	4.11	0.42	–	7.28

Table 6
Office building set-points.

Parameter	Value	Unit
Heating set-point	21	°C
Heating set-back	17	°C
Cooling set-point	26	°C
Max relative humidity winter	50	%
Max relative humidity summer	60	%

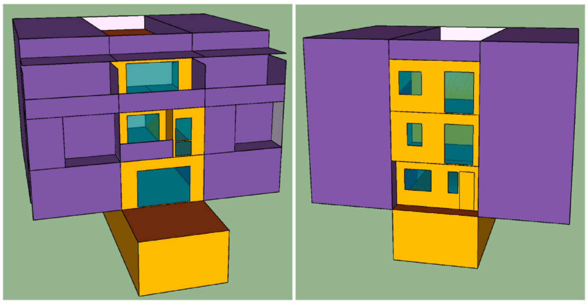

Fig. 6. Residential building, front view (left) and back view (right).

Table 7
Residential building geometric characteristics.

Parameter	Value
Ground floor surface	60.8 m^2
1st floor surface	60.7 m^2
2nd floor surface	53.8 m^2
Total surface	175.3 m^2
South façade surface	38.3 m^2
South façade window to wall ratio	47.5%
North façade surface	38.3 m^2
North façade window to wall ratio	29.1%

Table 8
Residential building envelope characteristics.

Climate	U [W/m^{2}K]	
	External wall	Roof
København	0.167	0.093
León	0.363	0.403
Almería	0.680	0.486
Bangalore	0.435	0.409
New Delhi	0.396	0.409

photovoltaic cell. Based on the laboratory and simulation data, two scenarios are considered. The first considers the scenario with the best average visible transparency (AVT) and colour rendering index (CRI), although with a lower efficiency of 3.46%. The second considers the scenario with the best efficiency of 5.54%, but with reduced AVT and CRI. Fig. 8 shows the transmittance of both cases of transparent PV glazing compared to a clear glass and a solar control glass. Note solar control properties of both PV glazing, with significantly reduced transmittance in the infrared.

The TPV glazing are implemented into glazing systems that fit the building regulation requirements of the selected locations.

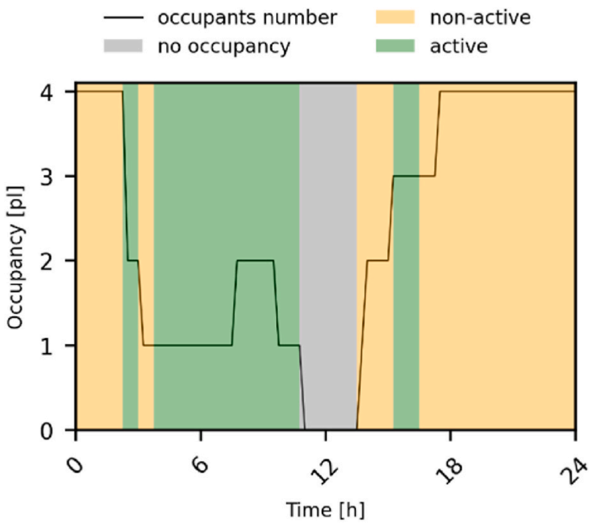

Fig. 7. Residential building example of occupancy daily stochastic schedule (sample of a specific working day).

Table 9
Residential heat gains and associated electricity consumption.

Type	Sensible gain	Radiative Fraction [−]	Latent gain [kg·s^{-1}·m^{-2}]	Electricity Consumption [W/m^2]
Equipment	2.2 W/m^2	0.7	–	2.2
People day	48.0 W/pl	0.6	20.0 W/pl	–
People night	27.6 W/pl	0.6	18.4 W/pl	–
Light	2 W/m^2	0.8	–	2.2

Table 10
Residential building set-points.

Parameter	Value	Unit
Heating set-point	20	°C
Heating set-back	15	°C
Cooling set-point	24.5	°C

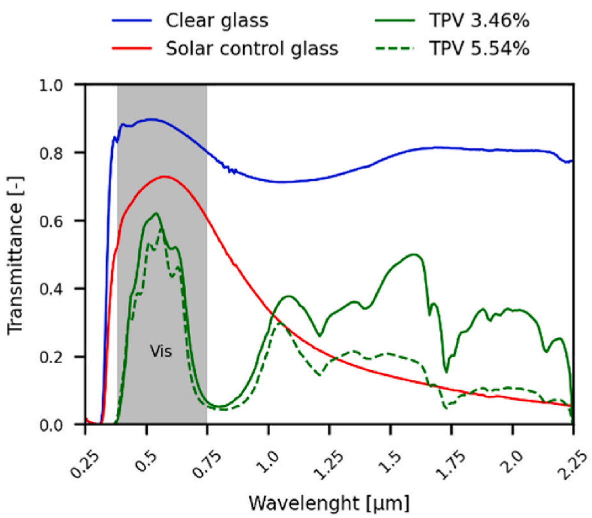

Fig. 8. TPV glazing transmittance compared to a clear glass and a solar control glass.

Table 11 summarizes the configurations and characteristics of the glazing systems in each location, including a reference "conventional" window and both of the TPV windows. The glazing system data is processed with WINDOW7 [52] software. The information of the conventional glass (float, low-e, and solar control glass) is obtained from the IGDB [53], while the spectral data of the TPV is obtained from the results of the Tech4win project [28] and processed with OPTICS6 [54].

As mentioned before, the economic analysis takes into account the cost of the reference conventional window in each location. The component and installation cost of the components are obtained from BEDEC construction materials database [55], as summarized in Table 12.

4. Result

4.1. Final energy use and energy balance

The final energy use and the energy balance of each scenario are shown in Figs. 9 and 10 for the office and residential buildings, respectively. First, the results highlight that the high internal gains of the office buildings reduce its heating load and increase its cooling load compared to the residential building. Hence, the office building is heating dominated in København and León, while the residential building also includes Almería as a heating dominated case. The two scenarios in India lead to cooling dominated cases in both buildings. Note that the relative change in energy use of the office building is lower than in the residential building. This is due to the higher share in ventilation and equipment energy use, which are unaffected by the BIPV windows performance.

Nevertheless, the BIPV windows result in an increase of the heating and lighting demand, related to the lower SHGC and visible transmittance compared to the conventional window in all scenarios. In contrast, the cooling is slightly reduced, with the exception of the New Delhi scenario, in which the PV windows do not improve the SHGC of the conventional ones.

In terms of total final energy use, the BIPV windows only present final energy use savings in specific cases. In the heating dominated scenarios, any increase in the heating demand and lighting demand offsets the decrease in cooling demand. In the cooling dominated scenarios, the decrease in the cooling demand is comparatively small to the increase in heating demand and lighting demand. As a result, only five PV window scenarios improve the final energy use compared to the conventional one: the office building in Almería, the office building in Bangalore (but only with the highest efficiency TPV cell case (5.54%)), and the residential building in Bangalore. In the other cases, the increase of heating and lighting final energy use offset the savings in cooling. Nevertheless, once accounting for the PV generation, all the scenarios present improved energy balances compared to the conventional windows.

However, it is relevant to notice that the energy balance compares the final energy use and the PV output, without taking into account the time coincidence. In the office building, the occupancy profile makes the energy use in the weekends to be close to zero. This means any PV generated cannot be used by the building immediately, hence it is exported. In the residential building, the peak of PV generation at noon usually concur with lower energy demand. As the study does not consider energy storage, this surplus of

Table 11
Configurations and characteristics of the glazing systems.

Loc.	Case	Configuration	U [W/m^{2}K]	SHGC [−]	T_{vis}[-]
København	Reference	13/12/6/12/8 float glass/argon/low-e glass/argon/low-e glass	0.999	0.514	0.554
	TPV 3.46%	14/16/6/16/8 TPV glass/argon/low-e glass/argon/low-e glass	0.808	0.235	0.247
	TPV 5.54%	14/16/6/16/8 TPV glass/argon/low-e glass/argon/low-e glass	0.808	0.207	0.210
León	Reference	14/12/8 float glass/air/low-e glass	1.653	0.492	0.526
	TPV 3.46%	14/12/6 TPV glass/air/low-e glass	1.653	0.306	0.272
	TPV 5.54%	14/12/6 TPV glass/air/low-e glass	1.653	0.276	0.231
Almería	Reference	13/12/8 float glass/air/float glass	2.553	0.587	0.544
	TPV 3.46%	14/12/6 TPV glass/air/float glass	2.554	0.382	0.276
	TPV 5.54%	14/12/6 TPV glass/air/float glass	2.554	0.341	0.235
Bangalore	Reference	13/12/9 Solar glass/air/float glass	1.606	0.334	0.410
	TPV 3.46%	14/12/9 TPV glass/air/float glass	2.554	0.382	0.276
	TPV 5.54%	14/12/9 TPV glass/air/float glass	2.554	0.341	0.235
New Delhi	Reference	13/16/9 Solar glass/air/float glass	1.460	0.269	0.294
	TPV 3.46%	14/16/9 TPV glass/air/float glass	2.470	0.380	0.276
	TPV 5.54%	14/16/9 TPV glass/air/float glass	2.470	0.338	0.235

Table 12
Conventional window cost per climate.

Window	Cost [€/m^2]
København	105.41
León	75.29
Almería	72.54
Bangalore	85.26
New Delhi	89.52

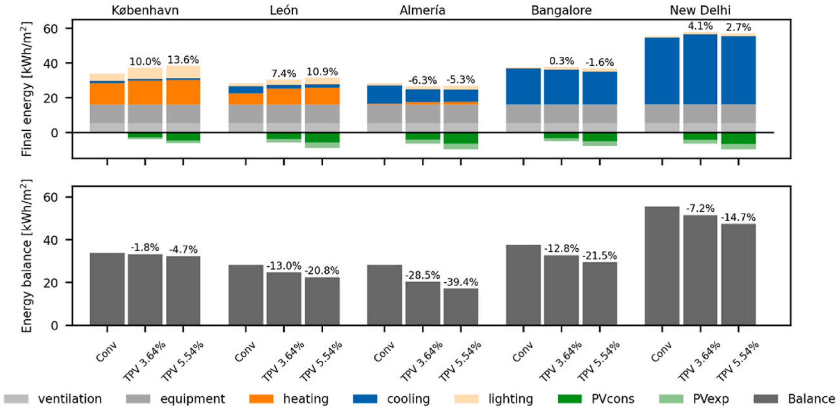

Fig. 9. Office building final energy and energy balance.

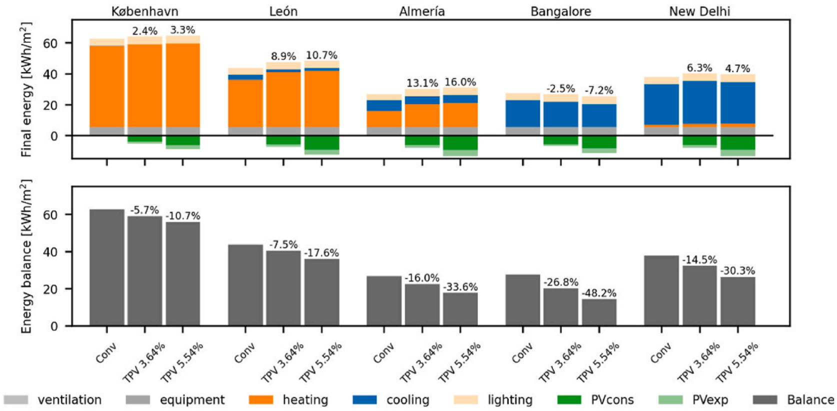

Fig. 10. Residential building final energy and energy balance.

electricity is considered to be exported to the grid. With the 3.46% efficiency cell the exported electricity amounts between 17-23% and 28–35% in the residential and office cases, respectively. With the 5.54% efficiency cell the exported electricity is between 26-32% and 29–36% in the residential and office cases, respectively. Note that the residential case has a significant increase in exported electricity when the efficiency raises, while the change is barely noticeable in the office building. This is related to the fact that electricity exports in the residential building are related to the peak production exceeding the demand. Hence, an increase in efficiency leads to larger peaks and more exported electricity. In contrast, the office building demands are high enough the exploit all the generated electricity during working days, but none of the PV generated in the weekends is exploited. Hence the ratio of exported electricity is related to the ratio of working and weekend day, but it is independent to efficiency in the studied cases.

4.2. Daylighting

In the case of the office building, the daylighting control implemented explains the low lighting electricity consumption shown in the previous section. The continuous lighting dimming allows consuming the minimum electricity required to maintain the illuminance set-point. This derives in a consumption probably lower than in a real building, but helps to highlight the impact of the windows characteristics. The PV windows have lower visible transparency than their conventional counterparts do, which results into lower daylighting illuminance values. Consequently, the occupancy time in which illuminance is below 500 lux increases, as shown in

Fig. 11. This explains the increase in lighting energy use. Nevertheless, the PV windows also decrease the time in which illuminance is above 2000 lux, potentially reducing the need of blinds and solar protections. As a result, the time within the useful daylighting illuminance (UDI) values (500–2000 lux) decreases for most of the PV window scenarios, with the exception of Almería and León.

In the case of the residential building, most of the occupancy is outside of day hours. Therefore, illuminance is below 200 lux most of the time users are active, as shown in Fig. 12. This minimizes the impact of PV window optical properties into the residential building lighting demand.

4.3. Economic evaluation

The PV windows payback sensitivity to CAPEX and average electricity price is presented in Figs. 13 and 14 for the office and residential buildings, respectively. The “y” axis of each box represents the average electricity price scenarios (El. price), which range between 0.05 and 0.55 €/kWh. This includes the current average electricity prices of the studied locations and a margin for increase, representing possible future scenarios. The dotted horizontal line represents the average electricity price of the corresponding location (0.28 €/kWh for Denmark, 0.23 €/kWh for Spain, and 0.08 €/kWh for India), according to Eurostat [56] and Statista [57] for data from 2019. The “x” axis represents the difference in CAPEX (CAPEX diff.) between the conventional reference window and the PV window. The CAPEX of conventional windows is expected to be between 70 and 110 €/m^2 for the studied cases, depending on configuration, and a commercial opaque BIPV solution can be in the range of 150 €/m^2. The CAPEX diff. range includes scenarios in which the PV windows is barely more expensive than a conventional one and below opaque BIPV solution, up to scenarios in which it will triple their prices. Finally, the expected lifetime of windows is 25 years. Hence the colour map presents in green the scenarios in which the payback is below the expected lifetime (economically feasible scenarios) and red for values above the minimum viable payback, with more intense colour meaning more difference from the 25 years threshold, while light yellow imply values close to it.

The results highlight that better energy balance (see Figs. 9 and 10) increase the possible scenarios in which the PV window will be feasible. Additionally, cooling dominated climates tend to have better results, requiring less improvement of the energy balance to achieve feasibility. This is related to sensible cooling demand tending to match the PV generation, hence the cooling dominated scenarios have better self-consumption results.

In any case, the most relevant result is the impact of electricity price schedule, which can greatly reduce the possible of scenarios in which the TPV windows are feasible. As shown in Figs. 15 and 16, The “current” scenarios awards the PV generation, which happens at the same time of “peak” or “flat” price period. In contrast, the “duck” chart scenario punishes the PV windows, as most of the PV generation occurs in the “supervalley” price, reducing the economic savings.

Note that the office building has less feasibility scenarios than the residential because of the operation regimes assumptions. The office building has no demand during the weekends. Hence, all the PV generated during nearly one third of the week is exported. Consequently, the office building case is more sensitive to the compensation scenario.

Compensation scenario may help making PV feasible in scenarios in which it has low energy balance improvement (see København in all scenarios, León and New Delhi in “duck” price schedules). However, in scenarios in which the PV provides a high improvement in the energy balance, the relevance of the compensation scenario is lower.

Finally, the results favour the PV window with better efficiency (5.52%), despite its lower visible transmittance and SHGC. The lower visible transmittance leads to an increase of lighting electricity demand. However, lighting in efficient building and good daylighting control is a small fraction of the total energy demand. Hence, this small increase is not significant. The lower SHGC is positive in cooling dominated climates, as it reduces the solar gains and, consequently the cooling load. In contrast, in cold climates, the lower SHGC reduces the contribution of solar gains to the heating, hence increasing the energy demand. Nevertheless, the SHGC and visible transmittance difference between the PV windows is small, especially compared to the conventional windows, thus the difference in PV efficiency (3.46% vs 5.52%) is the key parameter.

5. Discussion

The TPV glass prototypes considered in the study confer some solar control properties to the windows, due to its higher absorption

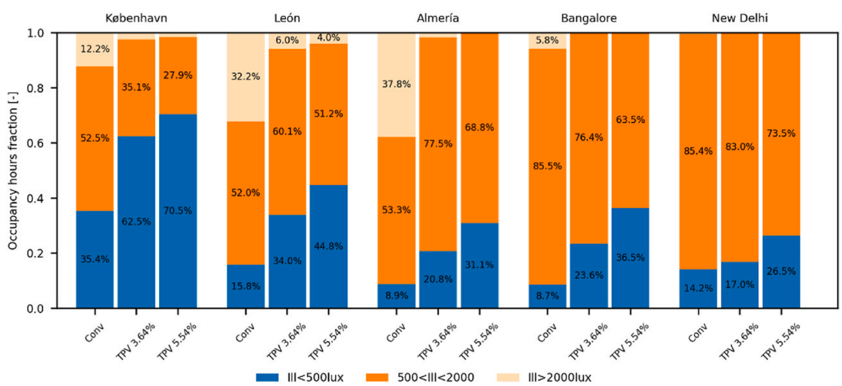

Fig. 11. Office building daylighting performance.

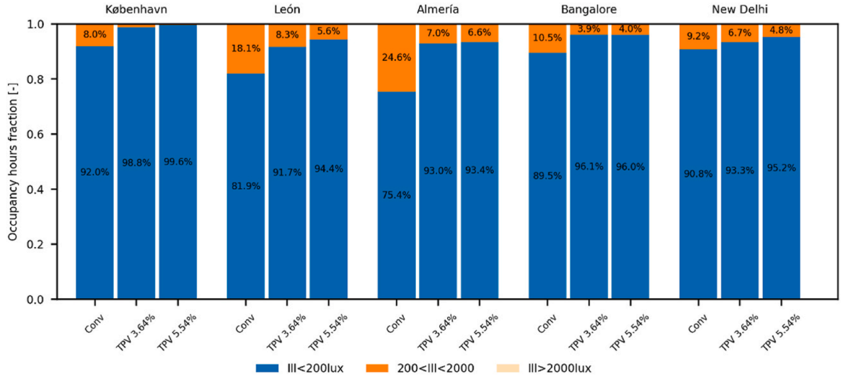

Fig. 12. Residential building daylighting performance.

in the IR and lower transmittance in the visible compared to clear glass. However, it does not have the same characteristics of the current solar control glazing in the market. As a result, in the climates that favour high solar gains to offset the heating loads, the PV windows will have lower solar heat gain coefficient (SHGC) than the conventional windows recommended for the location. On the other side, in hot climates that require minimizing the cooling loads, hence reduction of solar gains is necessary. In these case it may happen that the BIPV glazing studied does not provide as much solar protection as a reference solar control glass. Nevertheless, note that the PV effect effectively reduces the SHGC, although currently the window standards do not account for this effect yet [58].

In terms of energy use, the PV windows tend to increase the final energy demand of the building in almost all scenarios. In the cold cases, København and León, or scenarios with low internal gains (residential building), the lower SHGC results in an increase in the heating demand. For the cooling demand, the BIPV windows present savings in the cold (København) and mild (León and Almería) climates, as their SHGC is lower than that of the reference windows. In the hot India climates (H1 and H2) the differences in the SHGC between the studied BIPV windows and the reference window are lower, hence the impact is smaller and more variable. In all cases, the BIPV windows have lower visual transmittance, consequently increasing the lighting demand.

Despite the increase in final energy caused by the PV windows in many scenarios, their PV output makes a positive impact in the building energy balance in all the studied scenarios, with relative improvements from 2% (office building in København with lowest PV efficiency) up to 48% (residential building in Bangalore with highest PV efficiency). Yet, a significant fraction of the PV generations is exported to the grid, for the 5.52% efficiency window the exported fraction is between 29 and 36% in the office building and 27–32% in the residential, depending on the climate. In the office building case, the modelling assumptions make that all PV generation during the weekend results in exported electricity. In the residential case, the peak production happens at noon, usually in periods with less occupancy and energy demand. As a result, the feed-in tariff or investment in electricity storage will be relevant for the feasibility of the BIPV windows.

Consequently, the results highlight that the balance between optical, thermal, and efficiency characteristics of the PV window are key to determine its usefulness in different location, with heating dominated climates requiring higher PV efficiency in order to achieve positive energy balances and payback periods.

The results of the current article are consistent with those found in similar studies in the literature [10,15–27], although some discrepancies are found. Beyond the differences of climate, building characteristics, and type of PV window, all highlight the solar control properties of transparent PV and the lower visible transmittance. Consequently, the literature generally shows lower cooling demands but higher lighting and heating demands. Yet, the energy balance savings are usually higher than the values presented in the current article. One reason is the inclusion of equipment and ventilation energy use, which is not common in other articles and remains unaffected by the PV window. Nevertheless, the authors want to point at the different approach in the glazing system design and specially the selection of the reference window.

None of the reviewed studies considered a solar control window as reference, which are the business as usual solution for highly glazed building, especially in cooling dominated climates, but also in offices buildings in cold climates. Only a tinted glass with SHGC 0.501 was used by Zhang and Lu [16], while commercially available solar glass can easily reach 0.20 or 0.35 [59] with visible transmittance between 40 and 70%. These properties make conventional solar control glass to have SHGC in par (or better) with the BIPV windows presented in the literature, but with better visible transmittance. Also the thermal transmittance (U-value) between the reference and BIPV window present unfair comparisons, despite being a parameter not inherent of the PV window properties and easier to control. As example, Elhelali et al. [15] compared an a-Si glass ($U = 2.783$ W/m^{2}K, $SHGC = 0.367$, and $T_{vis} = 40\%$) to a single clear glass ($U = 6.121$ W/m^{2}K, $SHGC = 0.81$, and $T_{vis} = 88\%$) in Egypt. Uddin et al. [23] evaluate different insulated window solutions in different climates in China, but the thermal transmittance of the best conventional window (2.696–5.753 W/m^{2}K) is already worse than the worst PV window (1.145–2.667 W/m^{2}K). Raihan et al. [22] and Hassan et al. [27] use the same SHGC and T_{vis} for the BIPV and conventional window, but no counting the PV output in the latter.

Moreover, most of the studies just consider clear glass as reference, in some cases including a low-e glass in double pane configuration [27]. Additionally, single pane solutions are still considered [15,17,22,23,26,27] even in climates where its use is unwise, some examples are very cold cities such as Oslo [26,27] and Hothot [23]. Also, it is also common to use a use a single window solution

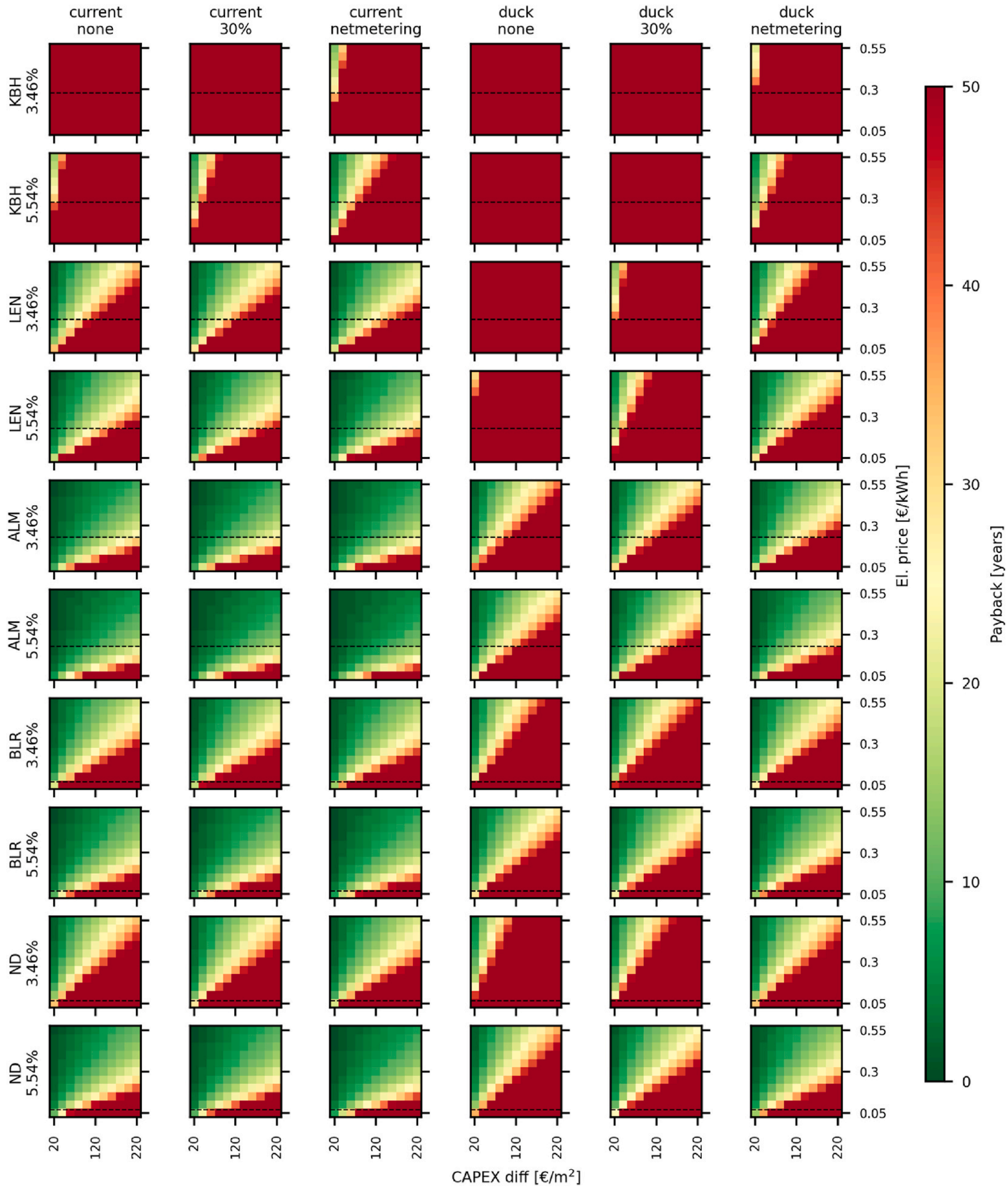

Fig. 13. Office building PV windows payback sensitivity to relative CAPEX and average electricity price.

for very different climates [16,25].

The current study uses as reference conventional windows that fulfil the building regulation requirements, showcasing energy savings lower than those reported in the literature. Note, the building regulations establish minimum energy efficiency requirements, but designers can aim for better performance values. Therefore, it is important to select carefully the reference conditions to estimate adequately the feasibility of PV windows.

In terms of economic evaluation, the electricity pricing schedules and the compensation scenarios will be key to promote the implementation of PV windows. The "duck" chart scenario encourages user to shift the energy consumption to periods with high availability of solar energy. However, it may de hamper the installation of distributed PV in buildings, especially for the less mature and lower efficiency transparent photovoltaics. The lowest electricity prices reduces the energy cost savings impact or the exported electricity incomes related to the BIPV generation. The investment cost difference (CAPEX diff. in the graph) is the other key parameter on the economic feasibility of the PV windows. This should not only include the window cost differences (glazing, frame, and installation costs), but all the related equipment. Hence, the PV case should include the inverters and other electrical equipment required. Moreover, the differences in solar control, daylighting control (shades), and artificial lighting equipment required to achieve

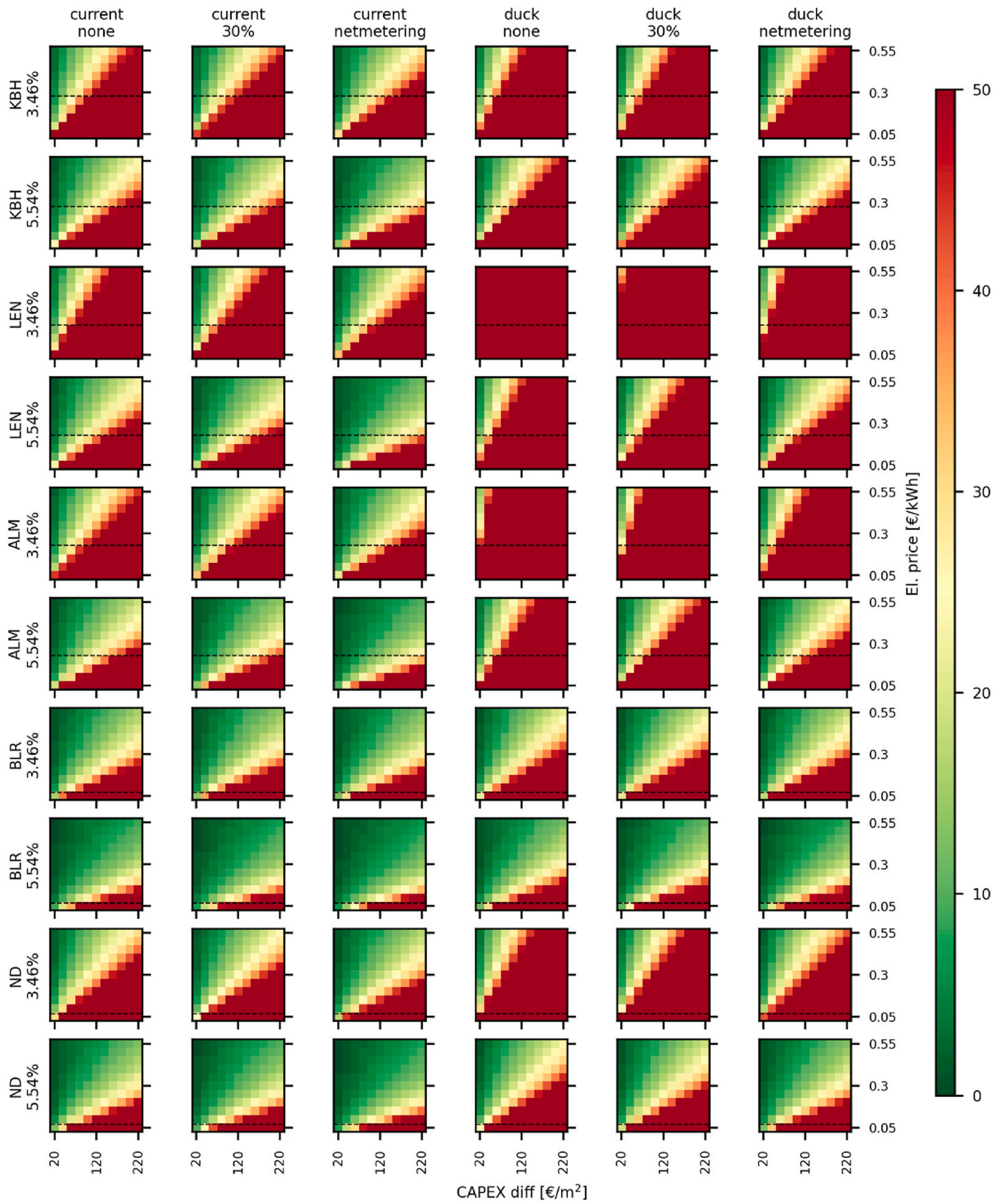

Fig. 14. Residential building PV windows payback sensitivity to relative CAPEX and average electricity price.

comfortable conditions in each solution should be taken into account. In order to limit the scope of the study, the present paper accounted only the glazing system differences. The results show that in the “current” electricity price schedules and average electricity price, the BIPV windows present the best performance on an office building in Almería location. There the conventional window is estimated to cost around 70 €/m^2 and the results show that even at CAPEX difference of 220 €/m^2 the PV window presents payback results below the expected lifetime. In both India locations, the payback maps presents many feasible scenarios. Yet, currently average electricity price are very low which significantly limits the feasibility of PV windows. In contrast, the København location showcase that PV windows in office building have very limited feasibility scenarios, although in the residential case with high PV efficiency and favourable compensation scenarios the number of feasible scenarios increase.

As mentioned before, the analysis of the impact of the PV windows is complex and multifactorial. The current study uses scenarios that directly compare the performance of the two prototype PV windows and reference windows, avoiding solar protection elements (landscape features, exterior elements such as overhangs and/or interior glare control systems such as adjustable louvers) and making control assumptions that may outperform a real building. The lighting consumption and visual comfort are the prime example. The lighting control used in the simulation presents an ideal performance that would minimize the consumption. Yet in a real case, the

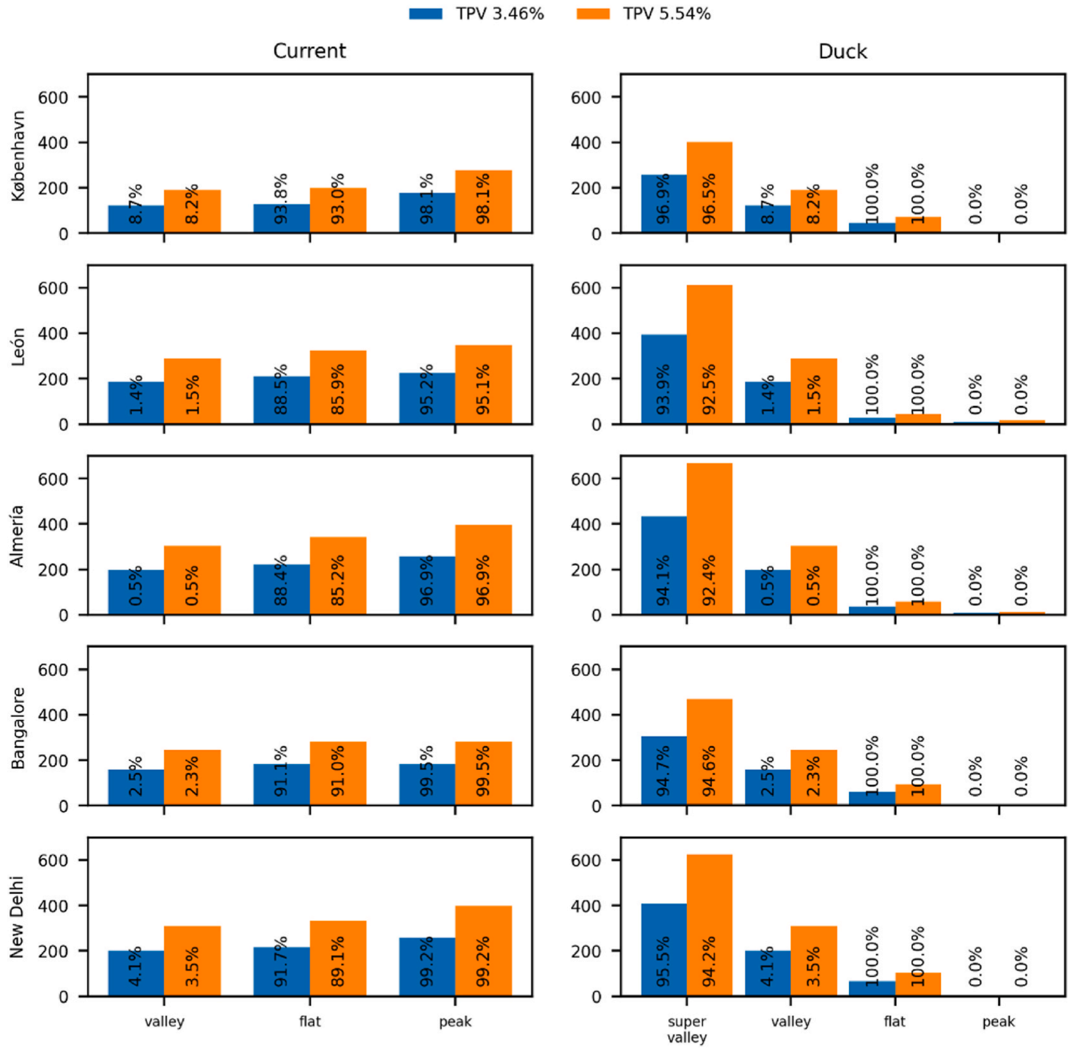

Fig. 15. Office PV generation (bars) and self-consumption fraction (percentages) per price slot.

capabilities of the sensors and the occupant behaviour will increase the lighting consumption. Hence, the differences between the reference and the PV windows will be lower. Moreover, in order to have good visual comfort, excessive illuminance and glare need to be minimized. In a real building that will imply the use of external or internal shading systems, which will change both the lighting and thermal performance of the building. As the results show that PV windows reduce the number of hours with excessive illuminance, this means a façade using conventional or PV windows will require different shading system for visual comfort, which will also affect in the investment cost for each solution. On top of that, the study presents results of reference residential and office buildings, while this are representative, the energy and economic values will depend on the geometry, orientation, location, and operation regimes of each specific case.

The study uses the properties of two prototypes of PV glazing. The data is obtained at laboratory level and two efficiency case scenarios, depending on upscaling losses, are assumed. In the conditions proposed, the PV glass with higher efficiency has clearly better results, yet the difference in optical and thermal properties is small. Moreover, the results also point to the difficulty of a PV glazing having properties adequate to all climates. In the present case, the PV glass have too low SHGC for the colder climates, in which PV output barely improves the energy balance and struggles to be economically feasible. In contrast, in the hotter climates the SHGC is not low enough, with the PV glazing solar control being subpar compared to actual solar control glass. Although in these cases the PV output makes favourable energy and economic scenarios. Nevertheless, the results and the capabilities of the simulation tool invite to study the combinations of optical, thermal, and efficiency combinations that make energy efficient PV glazing in different climates. Moreover, the study highlights the importance of considering window design that fits the building regulations, especially in order to design fair reference conventional windows.

Finally, the paper presents some good practices in BIPV window performance evaluation through selecting realistic reference windows. It also opens the discussion on the BIPV window economic evaluation, topic still lacking in this research area, by introducing

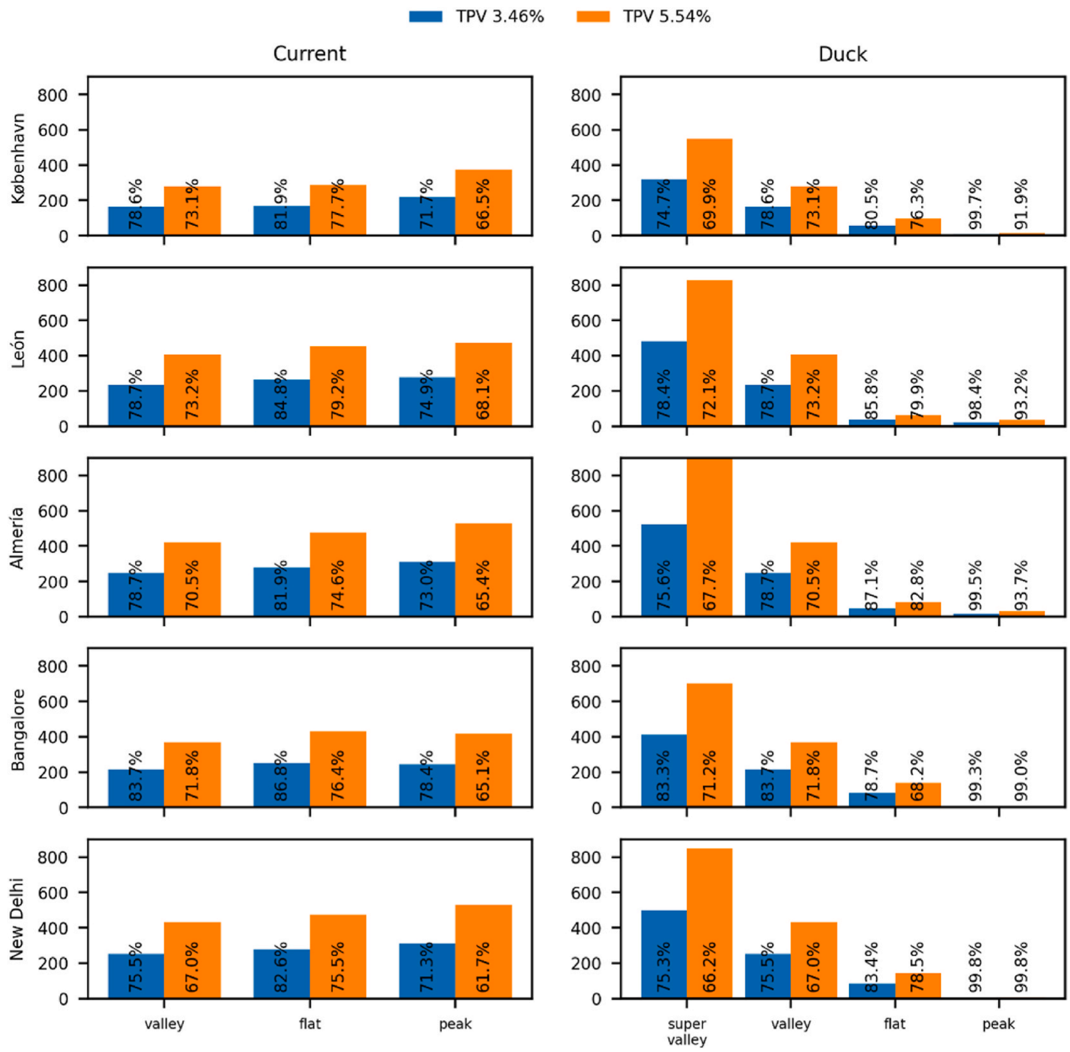

Fig. 16. Residential PV generation (bars) and self-consumption fraction (percentages) per price slot.

the impact of electricity pricing schedules and feed-in tariffs. Both topics will be key in the development and implementation of transparent BIPV windows. Other topics beyond the scope of the article, but also key into the research area, are the aforementioned comparison with external shading system (which may include photovoltaics too) and the visual comfort, which should consider the impact of the patterns and colours related to many transparent and semi-transparent PV cells. Also LCA studies must be carried out, following the positive results by Refs. [24,25] in terms of energy payback and energy return of investment.

6. Conclusions

The article presents a numeric study on the impact of two prototype photovoltaic transparent PV (TPV) glass on the performance of residential and office buildings. The simulation tool consist on a modified version of the TRNSYS18 multi-zone building (Type56) complex fenestration system (CFS) model, which allows including the PV effect in the window. The PV glass data is obtained from laboratory data, using assumptions for the upscaling efficiency losses.

The prototype PV windows used in the study have some solar control properties, although with a performance below actual solar control glass. Compared to the conventional windows adequate to a specific location, the PV windows cause an increase of the heating demand in cold climates and may increase the cooling demand in hot climates. Yet, the PV output is positive in all the scenarios considered, with the best results being in mild to warm climates. The work is limited to two PV glass prototypes, but the results already point that a right balance between thermal, optical, and efficiency properties is key to make energy efficient PV windows in each climate.

The economic feasibility is evaluated as a sensitivity study of payback. The parameters considered are the investment cost of the PV window, the average electricity price, and the electricity pricing schedules. The results highlight that electricity pricing schedules are key to the feasibility of the PV windows. In particular the “duck” chart encourages users to consume electricity during daylight hours, although it may refrain further installation of PV, especially less mature and lower efficiency technologies such as transparent PV. Nevertheless, the cases in which PV windows present good energy balance compared to the reference have a wider range of average electricity price and investment cost that make them economically feasible.

The main challenge of this study was to fulfil the building regulations by designing transparent PV windows that fit the requirements. Moreover, the analysis of commercially available conventional window showed many options outperformed the BIPV windows in terms of thermal-optical properties. This reduced the performance advantages of the BIPV, especially in very cold, where high SHGC are desirable, or very hot climates, where actual solar control windows outperform the BIPV window studied.

The existing literature on transparent BIPV windows already pointed the impact of the WWR and orientation of the windows, as well as the balance between the thermal, optical, and electrical characteristics. The current article highlights the need to select representative glazing systems designs that suit the building regulations requirements, as well as introduce key aspects on the economic evaluation. Further research on the topic must consider the integration of the BIPV window to the building façade design, accounting for alternatives including solar protection systems such as external shading, which may also integrate PV. The optical comfort and aesthetical acceptance must also be considered, as some of the innovative PV solutions might be colored or draw patterns in the windows. Some preliminary economic are present in the literature, but further studies are required to consider the whole façade design and the alternative transparent PV technologies. In addition, life cycle analysis have to be conducted beyond the energy payback or energy return of investment.

Author statement

Joaquim Romaní; Conceptualization, Methodology, Software, Validation, Data Curation, Writing Original Draft, Writing review and editing, Visualization. Alejandro Pérez-Rodríguez: Resources, Supervision, Project Administration, Funding Acquisition. Jaume Salom: Methodology, Resources, Writing Review, Supervision, Funding Acquisition.

Declaration of competing interest

The authors declare that they have no known competing financial interests or personal relationships that could have appeared to influence the work reported in this paper.

Data availability

Data will be made available on request.

Acknowledgements

This work has received funding from the European Union H2020 Framework Programme under Grant Agreement no. 826002 (Tech4Win). Joaquim Romaní would like to thank *Ministerio de Economía y Competitividad de España* for grant Juan de la Cierva FJC2018-038475-I.

Appendix A. Office building surfaces characteristics

Table A 1
Office building reference room walls envelope characteristics.

Surface	Parameters			Climates				
				København	León	Almería	Bangalore	New Delhi
External	Structure and thickness	Steel	m	0.002	0.002	0.002	0.002	0.002
		Mineral wool	m	0.21	0.12	0.05	0.14	0.14
		Aluminium	m	0.002	0.002	0.002	0.002	0.002
	U-value		$W/m^2{\cdot}K$	0.180	0.307	0.687	0.436	0.392
Partition	Structure and thickness	Steel	m	0.002	0.002	0.002	0.002	0.002
		Mineral wool	m	0.21	0.12	0.05	0.14	0.14
		Aluminium	m	0.002	0.002	0.002	0.002	0.002
	U-value		$W/m^2{\cdot}K$	0.180	0.307	0.687	0.436	0.392
Floor/ceiling slabs	Structure and thickness	Steel	m	0.002	0.002	0.002	0.002	0.002
		Mineral wool	m	0.21	0.12	0.05	0.14	0.14
		Aluminium	m	0.002	0.002	0.002	0.002	0.002
	U-value		$W/m^2{\cdot}K$	0.180	0.307	0.687	0.436	0.392

Appendix B. Residential building surfaces characteristics

Table B 1
Residential building surface characteristics for København.

Surface	Parameters				Climate
					København
External	Structure and thickness		Tiled concrete	m	0.11
			Insulation	m	0.2
			Brick	m	0.21
		U-value		$W/m^2 \cdot K$	0.175
External roof	Structure and thickness		Concrete	m	0.25
			Insulation	m	0.325
	U-value			$W/m^2 \cdot K$	0.115
Lateral wall	Structure and thickness		Gypsum	m	0.02
			Light perforated brick	m	0.14
			Gypsum	m	0.02
		U-value		$W/m^2 \cdot K$	1.874
Partition wall	Structure and thickness		Gypsum	m	0.02
			Light perforated brick	m	0.07
			Gypsum	m	0.02
		U-value		$W/m^2 \cdot K$	1.864
Floor slab	Structure and thickness		Gypsum	m	0.02
			Unidirectional concrete slab	m	0.2
			Cement mortar	m	0.04
			Stoneware tiles	m	0.02
		U-value		$W/m^2 \cdot K$	1.873

Table B 2
Residential building surface characteristics for Spain.

Surface	Parameters				Climate	
					León	Almería
External	Structure and thickness		Gypsum	m	0.02	0.02
			Light perforated brick	m	0.05	0.05
			Air chamber	m	0.05	0
			Extruded polysterene (XPS) insulation	m	0.075	0.025
			Perforated brick wall	m	0.14	0.14
			Lime mortar covering	m	0.02	0.21
		U-value		$W/m^2 \cdot K$	0.363	0.680
External roof	Structure and thickness		Gypsum	m	0.02	0.02
			Unidirectional concrete slab	m	0.2	0.2
			Extruded polysterene (XPS) insulation	m	0.09	0.05
			Cellular concrete slab	m	0.08	0.08
			Roofing tar/asphalt fabric	m	0.02	0.02
			Cement mortar	m	0.04	0.04
			Ceramic tiles	m	0.03	0.03
		U-value		$W/m^2 \cdot K$	0.324	0.486
Lateral wall	Structure and thickness		Gypsum	m	0.02	0.02
			Light perforated brick	m	0.14	0.14
			Gypsum	m	0.02	0.02
		U-value		$W/m^2 \cdot K$	1.874	1.874
Partition wall	Structure and thickness		Gypsum	m	0.02	0.02
			Light perforated brick	m	0.07	0.07
			Gypsum	m	0.02	0.02
		U-value		$W/m^2 \cdot K$	1.864	1.864
Floor slab	Structure and thickness		Gypsum	m	0.02	0.02
			Unidirectional concrete slab	m	0.2	0.2
			Cement mortar	m	0.04	0.04
			Stoneware tiles	m	0.02	0.02
		U-value		$W/m^2 \cdot K$	1.873	1.873

Table B 3
Residential building surface characteristics for India.

Surface	Parameters			Climate	
				Bangalore	New Delhi
External	Structure and thickness	Cement plaster	m	0.02	0.02

(*continued on next page*)

Table B 3 (*continued*)

Surface	Parameters			Climate	
				Bangalore	New Delhi
		Brick	m	0.2032	0.2032
		Air chamber	m	0.05	0.05
		Expanded ploystyrene	m	0.055	0.065
		Lime mortar covering	m	0.012	0.012
		U-value	$W/m^2 \cdot K$	0.445	0.395
External roof	Structure and thickness	Cement plaster	m	0.015	0.015
		Reinforced cement concrete (RCC)	m	0.15	0.15
		Bata coba brick	m	0.1	0.1
		Expanded ploystyrene	m	0.071	0.071
		Brick tile	m	0.03	0.03
		U-value	$W/m^2 \cdot K$	0.409	0.409
Lateral wall	Structure and thickness	Gypsum	m	0.02	0.02
		Light perforated brick	m	0.14	0.14
		Gypsum	m	0.02	0.02
		U-value	$W/m^2 \cdot K$	1.874	1.874
Partition wall	Structure and thickness	Gypsum	m	0.02	0.02
		Light perforated brick	m	0.07	0.07
		Gypsum	m	0.02	0.02
		U-value	$W/m^2 \cdot K$	1.864	1.864
Floor slab	Structure and thickness	Gypsum	m	0.02	0.02
		Unidirectional concrete slab	m	0.2	0.2
		Cement mortar	m	0.04	0.04
		Stoneware tiles	m	0.02	0.02
		U-value	$W/m^2 \cdot K$	1.873	1.873

References

[1] IPCC, Global Warming of 1.5 °C, 2018.
[2] IEA, Global Status Report for Buildings and Construction 2019 – Analysis, 2019. Paris (France).
[3] IEA, Tracking Buildings 2020 – Analysis, 2020. Paris (France).
[4] The European Commission, Directive 2010/31/EU on the Energy Performance of Buildings, 2010. Brussels (Belgium).
[5] The European Commission, Directive 2012/27/EU on Energy Efficiency, 2012.
[6] J. Apte, D. Arasteh, Y.J. Huang, Future advanced Windows for zero-energy homes, Build. Eng. 109 (2) (2003) 871–882.
[7] E. Biyik, et al., A key review of building integrated photovoltaic (BIPV) systems, Engineering Science and Technology, Int. J. 20 (3) (2017) 833–858.
[8] G. Quesada, D. Rousse, Y. Dutil, M. Badache, S. Hallé, A comprehensive review of solar facades. Transparent and translucent solar facades, Renew. Sustain. Energy Rev. 16 (5) (2012) 2643–2651.
[9] B.P. Jelle, C. Breivik, H. Drolsum Røkenes, Building integrated photovoltaic products: a state-of-the-art review and future research opportunities, Sol. Energy Mater. Sol. Cell. 100 (2012) 69–96.
[10] D.E. Attoye, K.A.T. Aoul, A. Hassan, A review on building integrated photovoltaic façade customization potentials, Sustainability 9 (12) (2017) 2287.
[11] J. Romaní, A. Ramos, J. Salom, Review of transparent and semi-transparent building-integrated photovoltaics for fenestration application modeling in building simulations, Energies 15 (2022) 3286.
[12] A. Heneman, BIPV: built-in solar energy, Renewable Energy Focus 9 (14) (2008) 16–19.
[13] I.S.E. Fraunhofer, Photovoltaics Report, Fraunhofer Institute for Solar Energy Systems: Freiburg, Germany, 2020.
[14] F. Martellotta, A. Cannavale, U. Ayr, Comparing Energy performance of different semi-transparent, building-integrated photovoltaic cells applied to "reference" buildings, Energy Proc. 126 (2017) 219–226.
[15] M. Elhelali, L. Elgizawi, S. Sheta, Thermal-lighting behavior using semi-transparent photovoltaic (STPV) windows for office spaces retrofit in Egypt, 0974-3154, Int. J. Eng. Res. Technol. 12 (2019) 936–941. Number 7.
[16] W. Zhang, L. Lu, Overall energy assessment of semi-transparent photovoltaic insulated glass units for building integration under different climate conditions, Renew. Energy 134 (2019) 818–827.
[17] Y. Cheng, M. Gao, J. Jia, Y. Sun, y. Fan, M. Yu, An optimal and comparison study on daylight and overall energy performance of double-glazed photovoltaics windows in cold region of China, Energy 170 (2019) 356–366.
[18] H. Musameh, H. Alreshidi, F. Al-Neami, W. Issa, Energy performance analytical review of semi-transparent photovoltaics glazing in the United Kingdom, J. Build. Eng. 54 (2022), 104686.
[19] Y. sun, K. Shanks, H. Baig, W. Zhang, X. Hao, Y. Li, B. He, R. Wilson, H. Liu, S. Sundaram, J. Zhang, L. Xie, T. Mallick, Y. Wu, Integrated semi-transparent cadmium telluride photovoltaic glazing into windows: energy and daylight performance for different architecture designs, Appl. Energy 231 (2018) 972–984.
[20] Y. Sun, K. Shanks, H. Baig, W. Zhang, X. Hao, Y. Li, He Bo, R. Wilson, H. Liu, S. Sundaram, J. Zhang, L. Xie, T. Mallic, Y. Wu, Integrated CdTe PV glazing into windows: energy and daylight performance for different window-to-wall ratio, Energy Proc. 158 (2019) 3014–3019.
[21] Y. Sun, D. Liu, J.F. Flor, K. Shank, H. Baig, R. Wilson, H. Liu, S. Sundaram, T.K. Mallick, Y. Wu, Analysis of the daylight performance of window integrated photovoltaics systems, Renew. Energy 145 (2020) 153–163.
[22] M.A. Raihan, K. Chattopadhyay, A. Bhatia, V. Garg, A.M. Hussain, Energy analysis of semi-transparent building integrated photovoltaic window in Hyderabad, India using automated parametric simulations, IOP Conf. Ser. Earth Environ. Sci. 1050 (2022), 012022.
[23] M.M. Uddin, C. Wang, C. Zhang, J. Ji, Investigating the energy-saving performance of a CdTe-based semi-transparent photovoltaic combined hybrid vacuum glazing window system, Energy 253 (2022), 124019.
[24] Z. Li, W. Zhang, L. Xie, W. Wang, H. Tian, M. Chen, J. Li, Life cycle assessment of semi-transparent photovoltaic window applied on building, J. Clean. Prod. 295 (2021), 126403.
[25] A. Anctil, E. Lee, R.R. Lunt, Net energy and cost benefit of transparent organic solar cells in building integrated applications, Appl. Energy 261 (2020), 114429.
[26] K.H. Refat, R.N. Sajjad, Prospect of achieving net-zero energy building with semi-transparent photovoltaics: a device to system level perspective, Appl. Energy 279 (2020), 115790.

[27] M.M. Hassan, K.H. Refat, M.Z. Baten, R.N. Sajjad, Energy saving potential of photovoltaic windows: impact of shading, geography and climate, Sol. Energy 240 (2022) 342–353.
[28] Tech4win, Disruptive Sustainable Technologies for Next Generation Pv Windows, 2019. http://www.tech4win.eu/. (Accessed 8 November 2022).
[29] M. Richet, N. Lemaitre, Emerging transparent IR organic photovoltaic devices for BIPV integration: status and challenges, in: Impressive and Tech4Win European projects Virtual Workshop on Transparent PV: Chall. Oppor., 2021, https://doi.org/10.5281/zenodo.514527.
[30] B. Vermang, G. Brammertz, A. López-Garcia, E. Saucedo, V. Izquierdo-Roca, P. Santilli, Development and optimization of UV filtering and UV selective PV devices, in: Impressive and Tech4Win European projects Virtual Workshop on Transparent PV: Chall. Opportu., 2021, https://doi.org/10.5281/zenodo.5145455.
[31] TESS. TRNSYS 18 (2017). https://www.trnsys.com/. (Accessed 8 November 2022).
[32] J. Romaní, M. Hiller, J. Salom, Modelling of transparent PV windows with complex fenestration systems in TRNSYS, in: Proceedings of the 17th IBPSA Conference, Bruges (Belgium), 2021, pp. 1649–1656.
[33] ISO 15099. Thermal Performance of Windows, Doors and Shading Devices – Detailed Calculations, International Organization for Standardization, 2003.
[34] TRANSSOLAR, TRNSYS 18 - a transient system simulation program, in: Multizone Building Modelling with Type56. University of Wisconsin-Madison: Madison Volume 5, 2018. Wisconsin (USA).
[35] J. Romaní, H. Szambolics, M. Jimenez, S. Calvo, A. Pérez-Rodríguez, J. Salom, Evaluation of the implementation of a BIPV glass in office buildings in Spain. SWC2021, Proc. ISES Solar World Congress (2021) 152–163.
[36] A. Nabil, J. Mardaljevic, Useful daylight illuminance: a new paradigm to access daylight in buildings, Light. Res. Technol. 37 (1) (2005) 41–59.
[37] C.F. Reinhart, J. Mardaljevic, Z. Rogers, Dynamic daylight performance metrics for sustainable building design, LEUKOS – J. illuminating Eng. Soc. North America 3 (1) (2006) 7–31.
[38] P. Denholm, M. O'Connell, G. Brinkman, J. Jorgenson. Overgeneration from Solar Energy in California: A Field Guide to the Duck Chart, NREL, 2015.
[39] SYNIKIA, D.2.1 Report on Design Plus Energy Neighbourhoods in Each of the Four Climatic Types, 2021.
[40] Danish Ministry of Transport, Building, and Housing. Executive order on building regulations 2018 (Br18). https://www.byggeriogenergi.dk/media/2202/danishbuildingregulations_2018_energy-requirements.pdf. (Accessed 8 November 2022).
[41] Código técnico de la edificación: Documento básico HE, Ahorro de energía. Ministerio de transportes, movilidad y agenda urbana, Ministerio de transportes, movilidad y agenda urbana, 2019.
[42] Bureau of Indian Standards. National Building Code of India, 2016.
[43] M. Kottek, J. Grieser, C. Beck, B. Rudolf, F. Rubel, World Map of the Köppen-Geiger climate classification updated, Meteorol. Z. 15 (2006) 259–263.
[44] Meteonorm 8. https://meteonorm.com/en/. (Accessed 8 November 2022).
[45] T. Péan, S. Ibañez-Iralde, J. Pascual, J. Salom, Design and test of reduced grey-box models adapted to office buildings, in: Proceedings of the 17th IBPSA Conference, Bruges (Belgium), 2021, pp. 1687–1694.
[46] ASHRAE. Handbook of Fundamentals, American Society of Heating, New York, 2017.
[47] J.A. Ortiz, Detailed Energy and Comfort Simulation of Integral Refurbishment of Existing Buildings in Catalonia, Ph.D. Thesis, Universitat Politècnica de Catalunya, Barcelona, 2016 (Spain).
[48] MARIE, Mediterranean Building Rethinking for Energy Efficiency Improvement Call for Proposal: 3rd Call, 2010. Agreement N° 1S-MED10-002.
[49] Episcope, TABULA WebTool. https://episcope.eu/building-typology/webtool/. (Accessed 8 November 2022).
[50] J. Ortiz, F. Guarino, J. Salom, C. Corchero, M. Cellura, Stochastic model for electrical loads in Mediterranean residential buildings: validation and applications, Energy Build. 80 (2014) 23–36, 0.
[51] Instituto Nacional de Estadística – España, Encuestas de Empleo del Tiempo 2009-2010, INE, 2010.
[52] Lawrence Berkeley National Laboratory, WINDOW7. https://windows.lbl.gov/software/window, 2022. (Accessed 8 November 2022).
[53] Lawrence Berkeley National Laboratory, International Glazing Data Base (IGDB), 2021. https://windows.lbl.gov/software/igdb. (Accessed 8 November 2022).
[54] Lawrence Berkeley National Laboratory, OPTICS6. https://windows.lbl.gov/software/optics, 2013. (Accessed 8 November 2022).
[55] BEDEC Proyecto y obra, Banco construcción 2021-01. https://metabase.itec.es/vide/es/bedec. (Accessed 8 November 2022).
[56] Eurostat, Electricity price statistics. https://ec.europa.eu/eurostat/statistics-explained/index.php?title=Electricity_price_statistics. (Accessed 23 December 2021).
[57] Statista. https://www.statista.com/topics/1323/energy-prices/. (Accessed 8 November 2022).
[58] S. Misara, N. Henze, A. Sidelev, A. Thermal Behaviours of BIPV-Modules (U-Value and g-Value), in: Proceedings of the 2^{6th} European Photovoltaic Solar Energy Conference and Exhibition, 26th EU PVSEC), Hamburg (Germany), 2011, pp. 4107–4115.
[59] Saint Gobain, Cool-lite SKN series – solar control glass. https://www.saint-gobain-glass.com/products/cool-lite-skn. (Accessed 8 November 2022).